

CircFNDC3B inhibits cell growth in abdominal aortic aneurysm by targeting the miR-1270/PDCD10 axis

Baoping Deng

Guilin Medical University Affiliated Hospital

Yue Wei

Shunde Women and Children's Hospital of Guangdong Medical University

Jinfeng Zhang

Shunde Women and Children's Hospital of Guangdong Medical University

Na Zeng

Shunde Women and Children's Hospital of Guangdong Medical University

Yulan He

Shunde Women and Children's Hospital of Guangdong Medical University

Qiaoli Zeng

Shunde Women and Children's Hospital of Guangdong Medical University

Dehua Zou

Shunde Women and Children's Hospital of Guangdong Medical University

Runmin Guo (✉ runminguo2020@163.com)

Shunde Women and Children's Hospital <https://orcid.org/0000-0001-6987-3051>

Jing Xu

Guilin Medical University Affiliated Hospital

Research article

Keywords: Abdominal aortic aneurysm, apoptosis, circRNA fibronectin type III domain containing 3B, miR-1270, programmed cell death 10, proliferation

Posted Date: June 16th, 2021

DOI: <https://doi.org/10.21203/rs.3.rs-622114/v1>

License:   This work is licensed under a Creative Commons Attribution 4.0 International License.

[Read Full License](#)

Abstract

Background

In certain cancers, circRNA fibronectin type III domain containing 3B (circFNDC3B) may serve as a specific target for the treatment. However, the role and underlying regulatory mechanisms of circFNDC3B in abdominal aortic aneurysm (AAA) remain unknown.

Materials

CircFNDC3B expression in AAA and normal tissues were assessed by qRT-PCR. The biological functions of circFNDC3B were evaluated by MTT, flow cytometry and Caspase-3 activity assays. Furthermore, the molecular mechanism of circFNDC3B was demonstrated by RNA immunoprecipitation (RIP), dual-luciferase reporter assay, western blotting, qRT-PCR and rescue experiments.

Results

We found that the expression of circFNDC3B was significantly upregulated in AAA clinical specimens. Functionally, overexpression of circFNDC3B inhibited vascular smooth muscle cell (VSMC) proliferation and induced apoptosis *in vitro*, yet, knockdown of circFNDC3B had the opposite effects. Mechanistically, circFNDC3B upregulated the expression of programmed cell death 10 (PDCD10) by acting as a molecular sponge for miR-1270. Notably, forced expression of PDCD10 countervailed the impact of circFNDC3B knockdown on AAA biological processes.

Conclusions

Our data indicated that circFNDC3B promoted the progression of AAA by targeting the miR-1270/PDCD10 pathway, and may be a potential therapeutic target in the treatment of AAA.

Background

Abdominal aortic aneurysm (AAA) is pathologic dilation of the infrarenal or abdominal aorta, proximal to the aortic bifurcation [1]. The incidence of new AAA diagnoses is as high as 40–67 per 100,000 person-years in Asian populations [2]. Often, AAA is asymptomatic but has high susceptibility to rupture [3]. The mortality following rupture of an aneurysm is as high as 50–80% [4]. At present, clinical intervention for AAA disease is limited to open surgical repair or less invasive endovascular repair for aneurysms larger than 5.5 cm, however, for aneurysms below 5.5 cm, no internal medicine treatment is available [4, 5]. Moreover, to date, there is no medical therapy to prevent the progression of AAA [6]. Therefore, it is important to better understand the underlying molecular mechanisms that participate in the formation and progression of AAA, and to develop novel therapeutic strategies for AAA patients.

Circular RNAs (circRNAs) are a new class of non-coding endogenous RNA characterized by a covalently closed loop structure without 5' to 3' polarity or a polyadenylated tail [7–9]. Compared to linear RNAs,

circRNAs have better stability and conservation [9, 10]. In recent years, numerous circRNAs have been implicated in multiple human diseases [11–14], including cancer, neurological diseases, and cardiovascular diseases. As a circRNA sheared from exons 5 and 6 of the FNDC3B gene, circRNA fibronectin type III domain containing 3B (circFNDC3B) has been shown to participate in modulating cardiac repair, restraining bladder carcinoma, and enhancing gastric and esophageal carcinoma [15–18]. A previous microarray study showed that circFNDC3B was highly expressed in AAA [19]. Still, the function and mechanism of circFNDC3B in AAA remains unclear.

The results of our study demonstrated a marked upregulation of circFNDC3B in AAA tissues, and that overexpression of circFNDC3B dramatically inhibited vascular smooth muscle cell (VSMC) proliferation and induced apoptosis via sponging miR-1270 to facilitate the expression of programmed cell death 10 (PDCD10). Our findings revealed a novel molecular mechanism underlying the circFNDC3B/miR-1270/PDCD10 axis in AAA progression.

Materials And Methods

Clinical tissue specimens

AAA clinical specimens and adjacent abdominal aortic normal tissues were acquired from 25 patients after surgical resection at Affiliated Hospital of Guilin Medical University (Guilin, China). All samples were snap frozen in liquid nitrogen, and stored at -80°C for further experimentation. Informed consent was obtained from all patients, and this study was approved by the Ethics Committee of Sun Yat-sen Memorial Hospital.

Cell culture

Human VSMCs, from Jennio Biotech (Guangzhou, China), were grown in medium containing smooth muscle growth supplements (Cascade Biologics, Karlsruhe, BW, Germany), 10% fetal bovine serum (FBS, Gibco-BRL, Grand Island, NY, USA), and the antibiotics penicillin G/streptomycin. Cells were incubated at 37°C with 5% CO₂.

Plasmid and transfection

The sequence of circFNDC3B was subcloned into the pCD5-ciR vector (Greenseed Biotech, Guangzhou, China) to construct the overexpression vectors for circFNDC3B. The circFNDC3B siRNA (sicircFNDC3B), PDCD10 siRNA (siPDCD10), and their negative control (NC) were obtained from Genechem (Shanghai, China), and miR-1270 and control mimics were purchased from RiboBio (Guangzhou, China). The sequences of oligonucleotides were used in the Table 1. VSMCs were transfected using Lipofectamine 2000 (Invitrogen, Carlsbad, CA, USA) according to the manufacturer's instructions.

Quantitative real-time polymerase chain reaction (qRT-PCR)

Genomic DNA (gDNA) from VSMCs was isolated using the QIAamp DNA Mini Kit (QIAGEN, Dusseldorf, NW, Germany). Total RNA from tissues and cells were purified using TRIzol Reagent (Invitrogen)

according to the manufacturer's manual. For miR-1270, mRNA was reverse transcribed into cDNA using Bulge-Loop™ microRNA specific RT-primers (RiboBio). For PDCD10 and circFNDC3B, mRNA was reverse transcribed into cDNA using random primers. Then, qRT-PCR was performed using the SYBR Green Mixture (Takara, Dalian, China) on an ABI 7900HT PCR System (Applied Biosystems, Foster City, CA, USA). The $2^{-\Delta\Delta C_t}$ method was used to calculate the relative expression. The primers were used in the Table 1.

RNase R Treatment

Two microgram of total RNA was treated with or without 3 U/mg of RNase R (Epicentre Technologies, Madison, Wisconsin, USA) at 37°C for 30 min. After treatment with or without RNase R, total RNA was reverse transcribed into cDNA using the PrimeScript RT reagent Kit (Takara, Dalian, China). Next, qRT-PCR was used to examine circFNDC3B and GAPDH mRNA expression levels.

MTT assay

Cells were seeded in 96-well plates at a density of 5000 cells/well. At the indicated time points (0, 24, 48, and 72h), 20 μ L MTT reagent (Sigma Aldrich, St. Louis, MO, USA) was added to each well and incubated for 4 h. Next, the media were removed and 100 μ L DMSO was added. The absorbance was examined at 490 nm with a microplate reader (Molecular Devices, Sunnyvale, CA, USA).

Flow cytometry assays

Cell cycle and apoptosis were detected using flow cytometry assays. For cell cycle analysis, cells were harvested and fixed with 70% ethanol at 4°C overnight. The fixed cells were incubated with RNase I and propidium iodide (PI; Sigma Aldrich) for 30 min in the dark and the cell cycle distribution was analyzed using flow cytometer (Becton Dickinson, Franklin Lakes, NJ, USA). For the apoptosis assay, cells were collected and stained with 5 μ L FITC-Annexin V (Roche, Basel, KB, Switzerland) and PI (Sigma Aldrich) for 30 min, and then analyzed using flow cytometry (Becton Dickinson).

Caspase-3 activity assay

The caspase-3 activity assay was conducted using caspase activity kits (Beyotime, Shanghai, China). The cells cultured in a 96-well plate were lysed and the cell lysates were collected. After centrifugation, the cell lysates were incubated with caspase-3 substrate in a black plate for 4 h, and then the absorbance was measured.

Dual-luciferase reporter assay

The 3'UTR of the PDCD10 and circFNDC3B cDNAs were inserted into a psiCHECK-2 vector, respectively (Promega, Madison, WI, USA) (PDCD10-3'UTR-wt or circFNDC3B-wt). The putative miR-1270 binding sequence was mutated using a QuikChange site-directed mutagenesis kit (Agilent Technologies, Santa Clara, CA, USA) (PDCD10-3'UTR-mut or circFNDC3B-mut). Cells were seeded in a 48-well plate at a density of 2.5×10^4 cells/well. After incubating for 24 hours, cells were co-transfected with PDCD10-3'UTR-wt

(mut), circFNDC3B-wt (mut) and miR-1270 or control mimics using Lipofectamine 2000 (Invitrogen). The luciferase activity was measured using a Dual Luciferase Assay Kit (Promega).

RNA immunoprecipitation (RIP)

An EZMagna RNA Immunoprecipitation (RIP) Kit (Millipore, Bedford, MA, USA) was used according to the manufacturer's instructions. Briefly, VSMCs cells were lysed with RIP lysis buffer. The extract was mixed with magnetic beads conjugated with anti-Ago2 or anti-IgG antibodies (Millipore) and incubated at 4°C for 6–8 hours. Next, the magnetic beads were washed with wash buffer and incubated with proteinase K at 55°C for 30 minutes. Finally, the purified RNA was subjected to qRT-PCR analysis.

Western blotting

Cells were lysed and total proteins were separated by sodium dodecyl sulfate-polyacrylamide gel electrophoresis (SDS-PAGE) and transferred to a polyvinylidene fluoride membrane (PVDF). Subsequently, the membrane was incubated with anti-PDCD10 (1:1000; Abcam, Cambridge, MA, USA) or anti-GAPDH (1:3000; Cell Signaling Technology, Beverly, MA, USA) primary antibodies overnight at 4°C, and then incubated for 2 h at room temperature with HRP-labeled secondary antibody (1:5000; Cell Signaling Technology). The blots were observed by chemiluminescence.

Statistical analysis

Data are expressed as the mean \pm standard deviation (SD). The differences between two groups were determined using Student's *t*-test. A *P* value < 0.05 was considered statistically significant.

Results

Identification of circFNDC3B and detection of its expression in AAA tissues

We discovered that circFNDC3B (hsa_circ_0006156) was derived from exon-5 and exon-6 of the FNDC3B gene locus and validated the sequence of circFNDC3B PCR products by Sanger Sequencing (Fig. 1a). Next, we designed two sets of primers for circFNDC3B. The convergent primers amplified the linear structure, and the divergent primers amplified the circular structure. The results demonstrated that the amplification of circFNDC3B only in cDNA, but not in gDNA (Fig. 1b). Moreover, we confirmed that circFNDC3B had a higher resistance to RNase R than the linear FNDC3B mRNA (Fig. 1c). The results of qRT-PCR analysis showed that the expression of circFNDC3B was significantly higher in clinical AAA specimens than in normal tissues (Fig. 1d). These results revealed that circFNDC3B was prominently increased in AAA tissues and may play an important role in the progression of AAA.

CircFNDC3B inhibits VSMC proliferation and promotes apoptosis

In view of the enhancement of circFNDC3B in AAA tissues, we explore the role of circFNDC3B in AAA by loss-of-function and gain-of-function experiments. We synthesized and transiently transfected siRNA targeting circFNDC3B or plasmids to decrease or increase the expression levels of circFNDC3B in VSMCs. The transfection efficiency was validated by qRT-PCR (Fig. 2a). The MTT assay exhibited that overexpression of circFNDC3B significantly suppressed the proliferation of VSMCs, while inhibition of circFNDC3B markedly increased their proliferation (Fig. 2b). Also, forced expression of circFNDC3B induced cell cycle arrest at the G0/G1 phase in VSMCs, whereas depletion of circFNDC3B promoted cell cycle progression from the G0/G1 phase to S phase (Fig. 2c). Moreover, the percentage of apoptotic cells were obviously increased by forced expression of circFNDC3B while reduced by circFNDC3B knockdown (Fig. 2d). Consistently, the caspase-3 activity in VSMCs was dramatically increased in circFNDC3B-overexpressing cells, but repressed in circFNDC3B knockdown cells (Fig. 2e). These results implied that circFNDC3B plays anti-proliferation and pro-apoptotic roles in VSMCs.

CircFNDC3B functions as a miR-1270 sponge in VSMCs

To explore the mechanism underlying the function of circFNDC3B in VSMCs, miR-1270 was predicted as a candidate target of circFNDC3B using the online software program circinteractome (Fig. 3a). A dual-luciferase reporter system was performed to verify the binding ability between miR-1270 and circFNDC3B. Luciferase activity was significantly decreased only with the co-transfection of circFNDC3B-wt and miR-1270 mimics (Fig. 3b). Meanwhile, in the RIP assay, circFNDC3B and miR-1270 were enriched in the Ago2 group (Fig. 3c). Additionally, miR-1270 expression was depressed by overexpression of circFNDC3B, while it was increased by knockdown of circFNDC3B (Fig. 3d). These results suggested that circFNDC3B could bind to miR-1270.

The effect of circFNDC3B on VSMC proliferation and apoptosis is reversed by miR-1270

Given that miR-1270 functioned as a target for circFNDC3B in VSMCs, we further checked on whether circFNDC3B exerts biological functions by miR-1270. Cells were co-transfected with circFNDC3B plasmid and miR-1270 mimics. As we expected, ectopical expression of miR-1270 partly overturned the inhibitory effect on proliferation and cell cycle progression of VSMCs mediated by circFNDC3B upregulation (Fig. 4a-b). Meanwhile, the acceleration of circFNDC3B overexpression on VSMC apoptosis was retarded with the upregulation of miR-1270 (Fig. 4c-d). These data suggested that miR-1270 could partially reverse the role of circFNDC3B in AAA.

PDCD10 expression is inhibited by circFNDC3B through sponging miR-1270

We predicted PDCD10 as the latent target of miR-1270 in VSMCs using the online microRNA-target program (TargetScan) (Fig. 5a). Luciferase reporter vectors including the wild type or mutant PDCD10 3'

untranslated region (3'UTR) were built, and co-transfected with miR-1270 or control mimics into VSMCs. The luciferase reporter activity of the wild type PDCD10 plasmid was dramatically decreased by miR-1270, however, the activity of the mutant PDCD10 vector made no difference (Fig. 5b). By western blotting and qRT-PCR analysis, ectopical expression of circFNDC3B significantly up-regulated PDCD10 protein and mRNA expression, which was subsequently decreased via miR-1270 overexpression in VSMCs cells (Fig. 5c-d). These data indicated that circFNDC3B inhibits the expression of PDCD10 by sponging miR-1270.

CircFNDC3B inhibits VSMC proliferation and enhances apoptosis via the miR-1270/PDCD10 axis To explore whether PDCD10 could affect circFNDC3B-regulated VSMC proliferation and apoptosis, cells were co-transfected with circFNDC3B plasmid and siPDCD10. We found that the upregulated expression of PDCD10 protein and mRNA resulted from circFNDC3B overexpression could be decreased by siPDCD10 (Fig. 6a-b). Furthermore, forced expression of circFNDC3B caused suppression of proliferation and cell cycle progression in VSMCs, while these inhibitory effects were abolished by silencing PDCD10 (Fig. 6c-d). In addition, the augmentation of apoptosis in circFNDC3B-elevated VSMCs was restored by PDCD10 knockdown (Fig. 6e-f). These findings provided evidence for the circFNDC3B/miR-1270/PDCD10 regulatory axis in VSMC apoptosis and proliferation.

Discussion

Previous research has shown that circFNDC3B shears from the FNDC3B gene of the FN3 family [20]. It has been reported that circFNDC3B is dysregulated in human cancers and acts as either a tumor suppressor or oncogene to regulate various biological processes, including cell proliferation, migration, and invasion. For instance, Chen et al. found that circFNDC3B was upregulated in renal carcinoma tissues, and that forced expression of circFNDC3B promoted cell viability, colony formation, and migration [21]. Wu et al. also reported that circFNDC3B was increased in papillary thyroid carcinoma tissues and cell lines, and that overexpression of circFNDC3B enhanced cell proliferation and promoted cell apoptosis *in vitro*, as well as facilitated papillary thyroid carcinoma progression *in vivo* [22]. On the contrary, research by Liu et al. showed that circFNDC3B was dramatically decreased in bladder cancer tissues, and resulted in restrained proliferation, migration, and invasion both *in vitro* and *in vivo* [16]. Similarly, circFNDC3B was downregulated in colon cancer cell lines and tissues, and inhibited cell viability, colony formation, invasion, and migration [23]. In our study, circFNDC3B was found to be highly expressed in AAA tissues. Ectopic expression of circFNDC3B repressed proliferation and accelerated apoptosis of VSMCs. However, knockdown of circFNDC3B accelerated proliferation and repressed apoptosis of VSMCs.

It has been found that circRNAs contain multiple selectively conserved miRNA target sites that could serve as miRNA sponges [24]. A study manifested that circCBFB mediated the expression of miR-28-5p to facilitate AAA [25], while another study showed that circCCDC66 facilitated proliferation and reduced apoptosis in VSMCs, but upregulated CCDC66 through its role as a miR-342-3p sponge [26]. Moreover, circFNDC3B inhibited bladder cancer progression via miR-1178-3p [16]. Hence, we assumed that

circFNDC3B might also work through competitively binding miRNA in AAA. In this study, dual-luciferase reporter and RIP assays were used to validate the direct interaction of circFNDC3B and miR-1270. qRT-PCR verified that circFNDC3B decreased the expression of miR-1270. Moreover, circFNDC3B affected cell proliferation and apoptosis in AAA by suppressing the expression of miR-1270, suggesting that circFNDC3B acts as a miR-1270 sponge in AAA.

Furthermore, miRNAs have been reported to bind to the 3'UTR of target messenger RNAs (mRNAs), causing either inhibition of translation efficiency or degradation of target mRNA [27]. To date, accumulating evidence suggests that circRNAs positively modulate the target genes of miRNAs. For example, circ-001971 contained a miR-29c-3p binding site and directly sponged miR-29c-3p to inhibit the expression of VEGFA [28]. Meanwhile, circTLK1 positively regulated the expression of CBX4 by sponging miR-136-5p [29]. Additionally, circSLC25A16 functioned as a miR-488-3p sponge to suppress HIF-1 α [30]. In this paper, we identified PDCD10 as a potential candidate gene of miR-1270 using online bioinformatic analysis. Further study confirmed that miR-1270 directly targeted the PDCD10 3'UTR and inhibited its expression. Moreover, qRT-PCR and western blotting analyses showed that PDCD10 was positively regulated by circFNDC3B via miR-1270.

Initially, PDCD10 was identified as TFAR15 (TF-1 cell apoptosis related gene-15), which is evolutionary conserved and is widely expressed in nearly all tissues [31]. PDCD10 is also named CCM3 because it is the third gene for cerebral cavernous malformations (CCMs) [32]. Increasing evidence has revealed a dual role of PDCD10 in various types of cells. PDCD10 knockdown inhibited breast cancer cell proliferation, growth, migration, and invasion *in vitro*, and also suppressed tumor growth and induced apoptosis *in vivo* [33]. Similarly, overexpression of PDCD10 significantly accelerated non-small cell lung cancer cell proliferation, migration and invasion, and also decreased apoptosis [34]. On the other hand, PDCD10 was downregulated in glioblastoma tissues, and knockdown of PDCD10 significantly stimulated cell proliferation, adhesion, migration and invasion, restrained apoptosis and caspase-3 activation, and facilitated tumor growth in a glioblastoma xenograft model [31, 35]. Ectopic PDCD10 expression led to inhibition of HUVEC proliferation, migration, and tube formation [36]. In our study, knockdown of PDCD10 could reverse the inhibition of cell proliferation and promotion of apoptosis caused by the overexpression of circFNDC3B. These results suggest that circFNDC3B promotes the progression of AAA by sponging miR-1270 to enhance PDCD10 expression.

Conclusions

In summary, we revealed the upregulation of circFNDC3B in human AAA tissues. We further verified that overexpression of circFNDC3B could inhibit cell proliferation and increase apoptosis by targeting the miR-1270/PDCD10 axis, suggesting a vital role for circFNDC3B in AAA. This affords the promise for a potential target in the clinical treatment of AAA.

Abbreviations

AAA: Abdominal aortic aneurysm; circRNAs: Circular RNAs; circFNDC3B: circRNA fibronectin type III domain containing 3B; VSMC: vascular smooth muscle cell; PDCD10: programmed cell death 10; NC: negative control; gDNA: Genomic DNA; RIP: RNA Immunoprecipitation; SDS-PAGE: sodium dodecyl sulfate-polyacrylamide gel electrophoresis; PVDF: polyvinylidene fluoride membrane; SD: mean \pm standard deviation; 3'UTR: 3' untranslated region; mRNAs: messenger RNAs; TF-1 cell apoptosis related gene-15: translation efficiency or TFAR15; CCMs: cerebral cavernous malformations.

Declarations

Acknowledgments

None.

Authors' contributions

All authors have read and approved the manuscript. BD made plans for the experiment. YW performed experiments. JZ and NZ supported their method. YH and QZ joined the discussion. DZ and RG wrote and revised the manuscript. JX collected and analyzed the data.

Funding

This study was jointly funded by the National Natural Science Foundation of China (81873649). The fund only provides funding and has no role in research design, data collection, analysis and interpretation, and writing manuscripts.

Availability of data and materials

The data used to support the findings of this study are available from the corresponding author upon request.

Ethics approval and consent to participate

This study was approved by the Ethics Committee of Sun Yat-sen Memorial Hospital (approval no: 57). All requirements of the Declaration of Helsinki were met. All patients provided written informed consent prior to their inclusion within the study.

Consent for publication

Not applicable.

Competing interests

The authors declare no conflicts of interest.

References

1. Johnston KW, Rutherford RB, Tilson MD, Shah DM, Hollier L, Stanley JC. Suggested standards for reporting on arterial aneurysms. Subcommittee on Reporting Standards for Arterial Aneurysms, Ad Hoc Committee on Reporting Standards, Society for Vascular Surgery and North American Chapter, International Society for Cardiovascular Surgery. *J Vasc Surg.* 1991;13(3):452–8.
2. Salem MK, Rayt HS, Hussey G, Rafelt S, Nelson CP, Sayers RD, Naylor AR, Nasim A. Should Asian men be included in abdominal aortic aneurysm screening programmes? *Eur J Vasc Endovasc Surg.* 2009;38(6):748–9.
3. Brewster DC, Cronenwett JL, Hallett JW Jr, Johnston KW, Krupski WC, Matsumura JS, Joint Council of the American Association for Vascular S. Society for Vascular S. Guidelines for the treatment of abdominal aortic aneurysms. Report of a subcommittee of the Joint Council of the American Association for Vascular Surgery and Society for Vascular Surgery. *J Vasc Surg.* 2003;37(5):1106–17.
4. Li Y, Wang W, Li L, Khalil RA. MMPs and ADAMs/ADAMTS inhibition therapy of abdominal aortic aneurysm. *Life Sci.* 2020;253:117659.
5. Lu H, Sun J, Liang W, Chang Z, Rom O, Zhao Y, Zhao G, Xiong W, Wang H, Zhu T, et al. Cyclodextrin Prevents Abdominal Aortic Aneurysm via Activation of Vascular Smooth Muscle Cell TFEB. *Circulation.* 2020.
6. Cooper HA, Cicalese S, Preston KJ, Kawai T, Okuno K, Choi ET, Kasahara S, Uchida HA, Otaka N, Scalia R, et al. Targeting Mitochondrial Fission as a Potential Therapeutic for Abdominal Aortic Aneurysm. *Cardiovasc Res.* 2020.
7. Guo JU, Agarwal V, Guo H, Bartel DP. Expanded identification and characterization of mammalian circular RNAs. *Genome Biol.* 2014;15(7):409.
8. Barrett SP, Wang PL, Salzman J. Circular RNA biogenesis can proceed through an exon-containing lariat precursor. *Elife.* 2015;4:e07540.
9. Memczak S, Jens M, Elefsinioti A, Torti F, Krueger J, Rybak A, Maier L, Mackowiak SD, Gregersen LH, Munschauer M, et al. Circular RNAs are a large class of animal RNAs with regulatory potency. *Nature.* 2013;495(7441):333–8.
10. Jeck WR, Sorrentino JA, Wang K, Slevin MK, Burd CE, Liu J, Marzluff WF, Sharpless NE. Circular RNAs are abundant, conserved, and associated with ALU repeats. *RNA (New York, NY).* 2013; 19(2):141–157.
11. Deng W, Peng W, Wang T, Chen J, Qiu X, Fu L, Zhu S. Microarray profile of circular RNAs identifies hsa_circRNA_102459 and hsa_circRNA_043621 as important regulators in oral squamous cell carcinoma. *Oncol Rep.* 2019;42(6):2738–49.
12. Shen F, Liu P, Xu Z, Li N, Yi Z, Tie X, Zhang Y, Gao L. CircRNA_001569 promotes cell proliferation through absorbing miR-145 in gastric cancer. *J Biochem.* 2019;165(1):27–36.

13. Wu H, Wu S, Zhu Y, Ye M, Shen J, Liu Y, Zhang Y, Bu S. Hsa_circRNA_0054633 is highly expressed in gestational diabetes mellitus and closely related to glycosylation index. *Clin Epigenetics*. 2019;11(1):22.
14. Zhou ZB, Huang GX, Fu Q, Han B, Lu JJ, Chen AM, Zhu L. circRNA.33186 Contributes to the Pathogenesis of Osteoarthritis by Sponging miR-127-5p. *Mol Ther*. 2019;27(3):531–41.
15. Luo G, Li R, Li Z. CircRNA circFNDC3B promotes esophageal cancer progression via cell proliferation, apoptosis, and migration regulation. *Int J Clin Exp Pathol*. 2018;11(8):4188–96.
16. Liu H, Bi J, Dong W, Yang M, Shi J, Jiang N, Lin T, Huang J. Invasion-related circular RNA circFNDC3B inhibits bladder cancer progression through the miR-1178-3p/G3BP2/SRC/FAK axis. *Mol Cancer*. 2018;17(1):161.
17. Hong Y, Qin H, Li Y, Zhang Y, Zhuang X, Liu L, Lu K, Li L, Deng X, Liu F, et al. FNDC3B circular RNA promotes the migration and invasion of gastric cancer cells via the regulation of E-cadherin and CD44 expression. *J Cell Physiol*. 2019;234(11):19895–910.
18. Garikipati VNS, Verma SK, Cheng Z, Liang D, Truongcao MM, Cimini M, Yue Y, Huang G, Wang C, Benedict C, et al. Circular RNA CircFndc3b modulates cardiac repair after myocardial infarction via FUS/VEGF-A axis. *Nat Commun*. 2019;10(1):4317.
19. Zhou M, Shi Z, Cai L, Li X, Ding Y, Xie T, Fu W. Circular RNA expression profile and its potential regulative role in human abdominal aortic aneurysm. *BMC Cardiovasc Disord*. 2020;20(1):70.
20. Syed A, Lukacsovich T, Pomeroy M, Bardwell AJ, Decker GT, Waymire KG, Purcell J, Huang W, Gui J, Padilla EM, et al. Miles to go (mtgo) encodes FNDC3 proteins that interact with the chaperonin subunit CCT3 and are required for NMJ branching and growth in *Drosophila*. *Dev Biol*. 2019;445(1):37–53.
21. Chen T, Yu Q, Shao S, Guo L. Circular RNA circFNDC3B protects renal carcinoma by miR-99a downregulation. *J Cell Physiol*. 2020;235(5):4399–406.
22. Wu G, Zhou W, Pan X, Sun Z, Sun Y, Xu H, Shi P, Li J, Gao L, Tian X. Circular RNA Profiling Reveals Exosomal circ_0006156 as a Novel Biomarker in Papillary Thyroid Cancer. *Mol Ther Nucleic Acids*. 2020;19:1134–44.
23. Pan Z, Cai J, Lin J, Zhou H, Peng J, Liang J, Xia L, Yin Q, Zou B, Zheng J, et al. A novel protein encoded by circFNDC3B inhibits tumor progression and EMT through regulating Snail in colon cancer. *Mol Cancer*. 2020;19(1):71.
24. Hansen TB, Jensen TI, Clausen BH, Bramsen JB, Finsen B, Damgaard CK, Kjems J. Natural RNA circles function as efficient microRNA sponges. *Nature*. 2013;495(7441):384–8.
25. Yue J, Zhu T, Yang J, Si Y, Xu X, Fang Y, Fu W. CircCBFB-mediated miR-28-5p facilitates abdominal aortic aneurysm via LYPD3 and GRIA4. *Life Sci*. 2020:117533.
26. Yang R, Wang Z, Meng G, Hua L. Circular RNA CCDC66 facilitates abdominal aortic aneurysm through the overexpression of CCDC66. *Cell Biochem Funct*. 2020.
27. Huang Y, Shen XJ, Zou Q, Wang SP, Tang SM, Zhang GZ. Biological functions of microRNAs: a review. *J Physiol Biochem*. 2011;67(1):129–39.

28. Chen C, Huang Z, Mo X, Song Y, Li X, Li X, Zhang M. The circular RNA 001971/miR-29c-3p axis modulates colorectal cancer growth, metastasis, and angiogenesis through VEGFA. *J Exp Clin Cancer Res.* 2020;39(1):91.
29. Li J, Huang C, Zou Y, Ye J, Yu J, Gui Y. CircTLK1 promotes the proliferation and metastasis of renal cell carcinoma by sponging miR-136-5p. *Mol Cancer.* 2020;19(1):103.
30. Shangguan H, Feng H, Lv D, Wang J, Tian T, Wang X. Circular RNA circSLC25A16 contributes to the glycolysis of non-small-cell lung cancer through epigenetic modification. *Cell Death Dis.* 2020;11(6):437.
31. Lambertz N, El Hindy N, Kreitschmann-Andermahr I, Stein KP, Dammann P, Oezkan N, Mueller O, Sure U, Zhu Y. Downregulation of programmed cell death 10 is associated with tumor cell proliferation, hyperangiogenesis and peritumoral edema in human glioblastoma. *BMC Cancer.* 2015;15:759.
32. Yang YJ, Liu ZS, Lu SY, Li C, Hu P, Li YS, Liu NN, Tang F, Xu YM, Zhang JH, et al. Molecular cloning, expression and characterization of programmed cell death 10 from sheep (*Ovis aries*). *Gene.* 2015;558(1):65–74.
33. Tan P, Ye Y, He L, Xie J, Jing J, Ma G, Pan H, Han L, Han W, Zhou Y. TRIM59 promotes breast cancer motility by suppressing p62-selective autophagic degradation of PDCD10. *PLoS Biol.* 2018;16(11):e3000051.
34. Yang D, Wang JJ, Li JS, Xu QY. miR-103 Functions as a Tumor Suppressor by Directly Targeting Programmed Cell Death 10 in NSCLC. *Oncol Res.* 2018;26(4):519–28.
35. Nickel AC, Wan XY, Saban DV, Weng YL, Zhang S, Keyvani K, Sure U, Zhu Y. Loss of programmed cell death 10 activates tumor cells and leads to temozolomide-resistance in glioblastoma. *J Neurooncol.* 2019;141(1):31–41.
36. Gao Y, Yin Y, Xing X, Zhao Z, Lu Y, Sun Y, Zhuang Z, Wang M, Ji W, He Y. Arsenic-induced anti-angiogenesis via miR-425-5p-regulated CCM3. *Toxicol Lett.* 2016;254:22–31.

Tables

Due to technical limitations, table 1 is only available as a download in the Supplemental Files section.

Figures

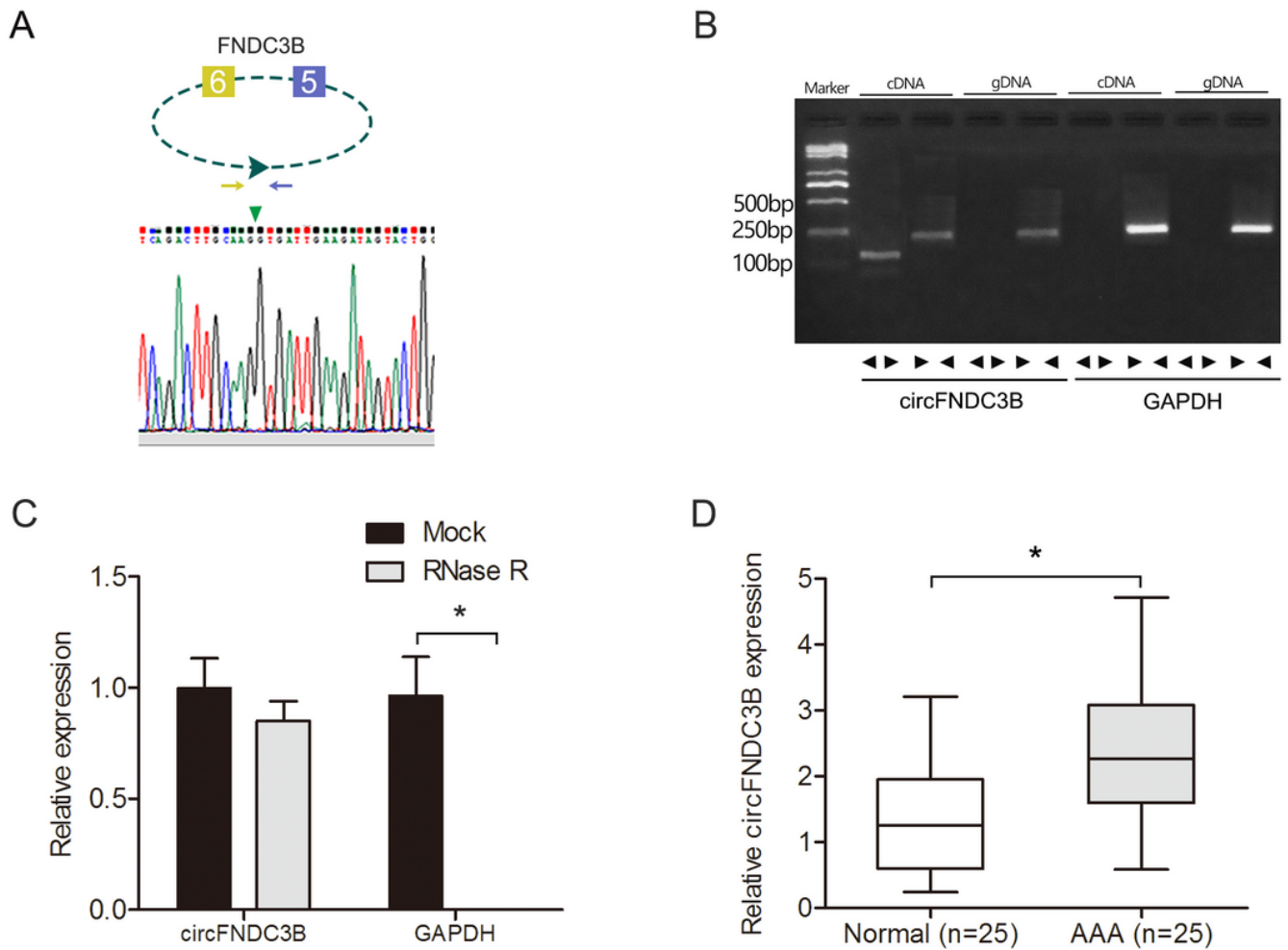


Figure 1

Identification of circFNDC3B and detection of its expression in AAA tissues. a Schematic diagram showing that circFNDC3B consists of FNDC3B exon-5 and exon-6. The sequence of circFNDC3B was confirmed by Sanger sequencing. b Divergent primers amplified circFNDC3B in cDNA but not in gDNA. c The stability of circFNDC3B in response to RNase R. d The expression of circFNDC3B in clinical AAA tissues and normal tissues as detected by qRT-PCR. Values represent the mean \pm SD (n = 3 per group). *p < 0.05.

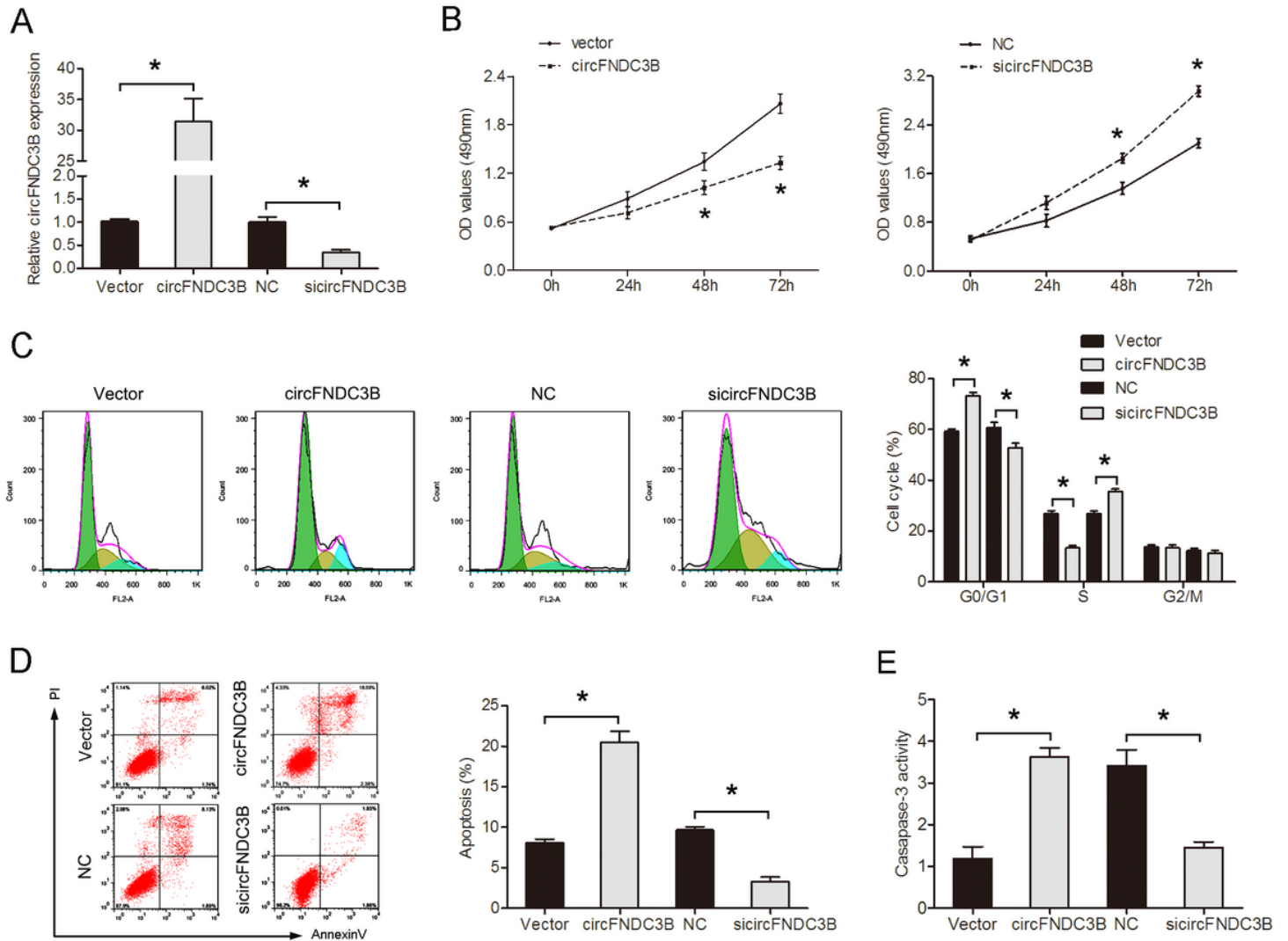


Figure 2

CircFNDC3B inhibits VSMC proliferation and promotes apoptosis. a VSMCs were transfected with circFNDC3B plasmid or sircFNDC3B. The expression of circFNDC3B was detected by qRT-PCR. b Cell proliferation was detected by MTT assay. c Cell cycle progression was examined by flow cytometry assay. d Cell apoptosis was examined by flow cytometry and caspase-3 activity assays. Values represent the mean \pm SD (n = 3 per group). *p < 0.05.

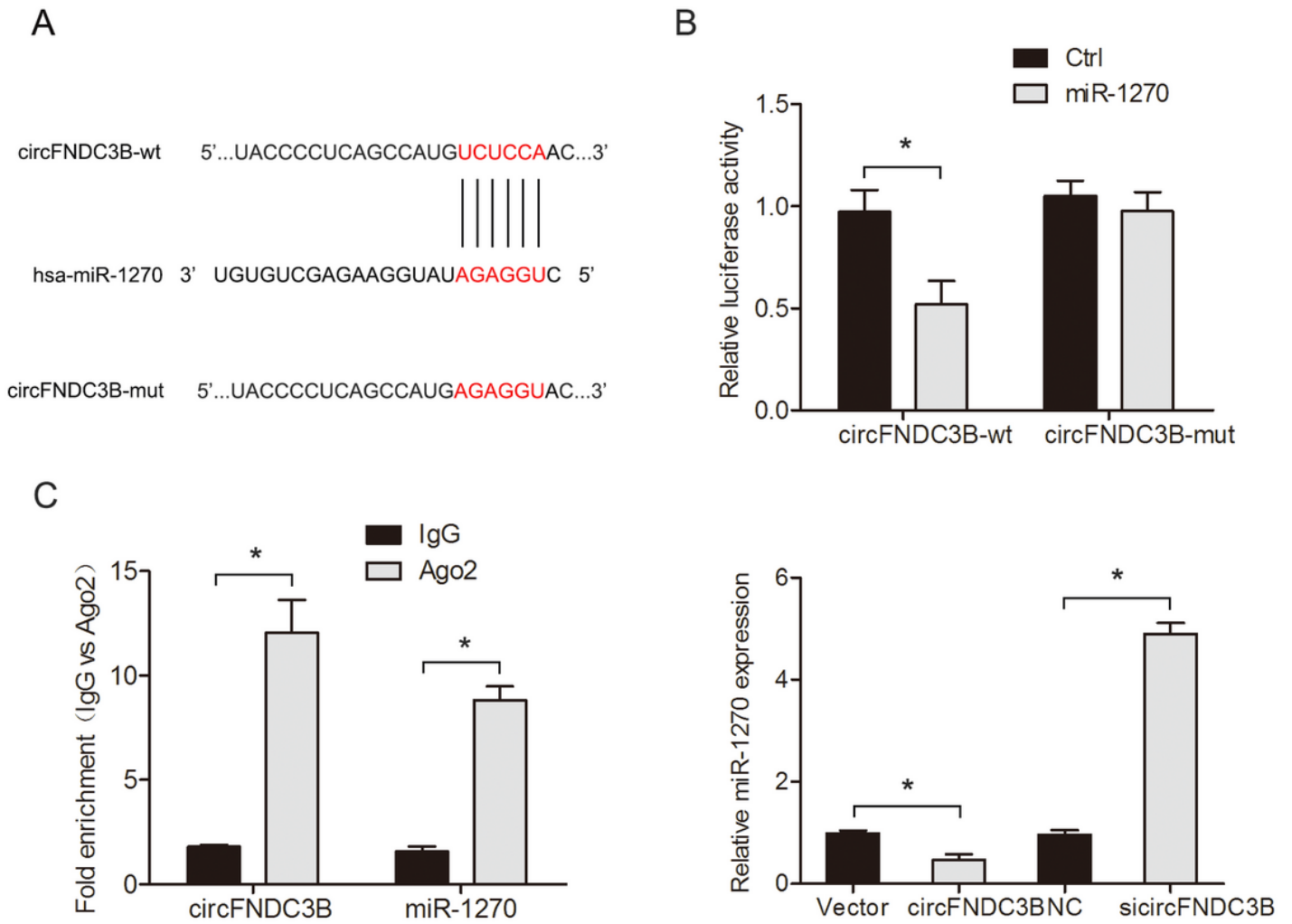


Figure 3

CircFNDC3B functions as a miR-1270 sponge in VSMCs. a The binding site between circFNDC3B and miR-1270. b The binding ability between miR-1270 and circFNDC3B was confirmed by dual-luciferase reporter assay. c A RIP assay was established to assess the combination of circFNDC3B and miR-1270. d MiR-1270 levels were measured by qRT-PCR. Values represent the mean \pm SD (n = 3 per group). *p < 0.05.

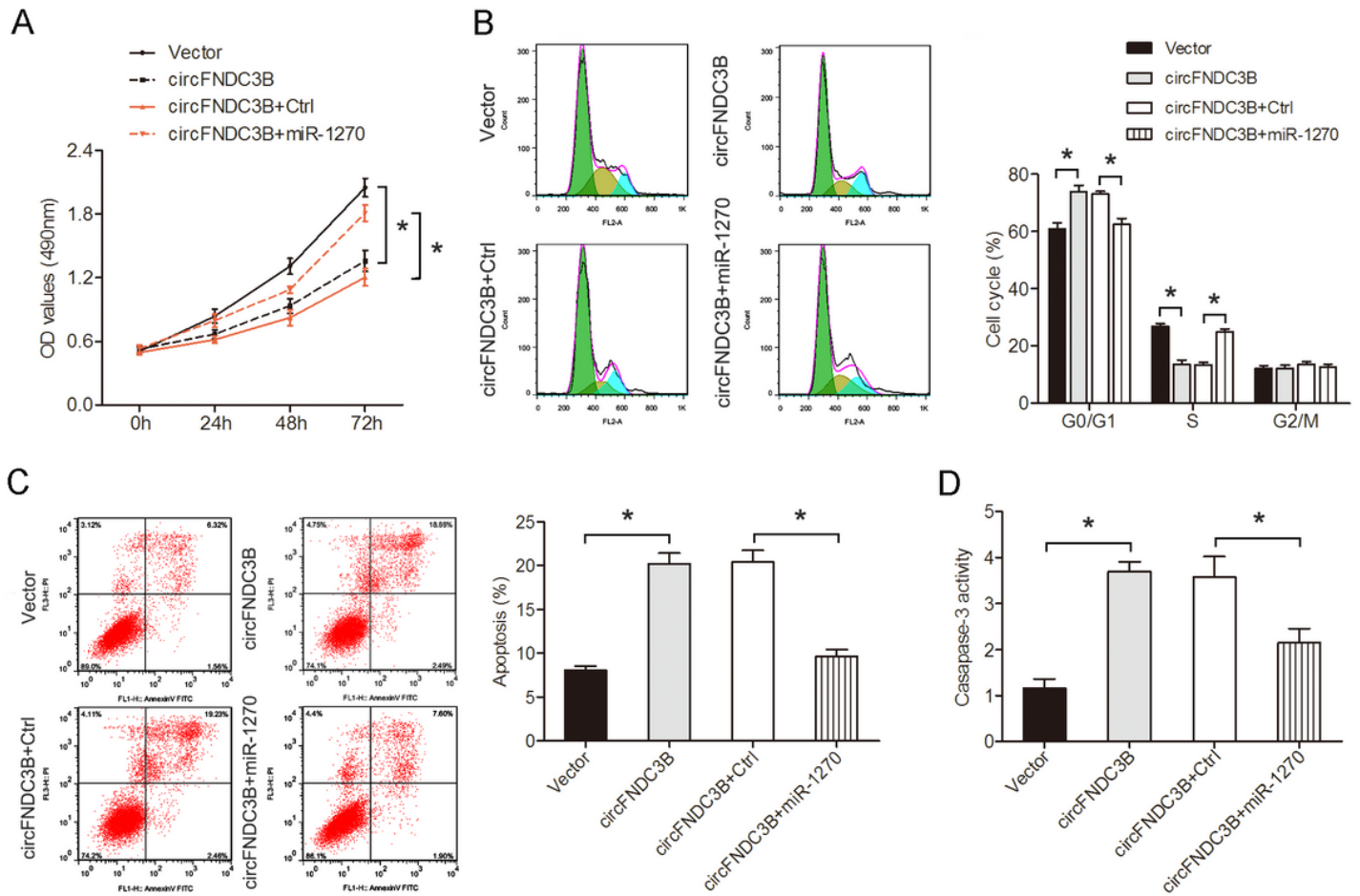


Figure 4

The effect of circFNDC3B on VSMC proliferation and apoptosis is reversed by miR-1270. a VSMCs were co-transfected with circFNDC3B plasmid and miR-1270 mimics and proliferation were assessed by MTT assay. b Cell cycle progression in VSMCs was examined by flow cytometry. c-d VMSC apoptosis was evaluated by flow cytometry and caspase-3 activity assays. Values represent the mean \pm SD (n = 3 per group). *p < 0.05.

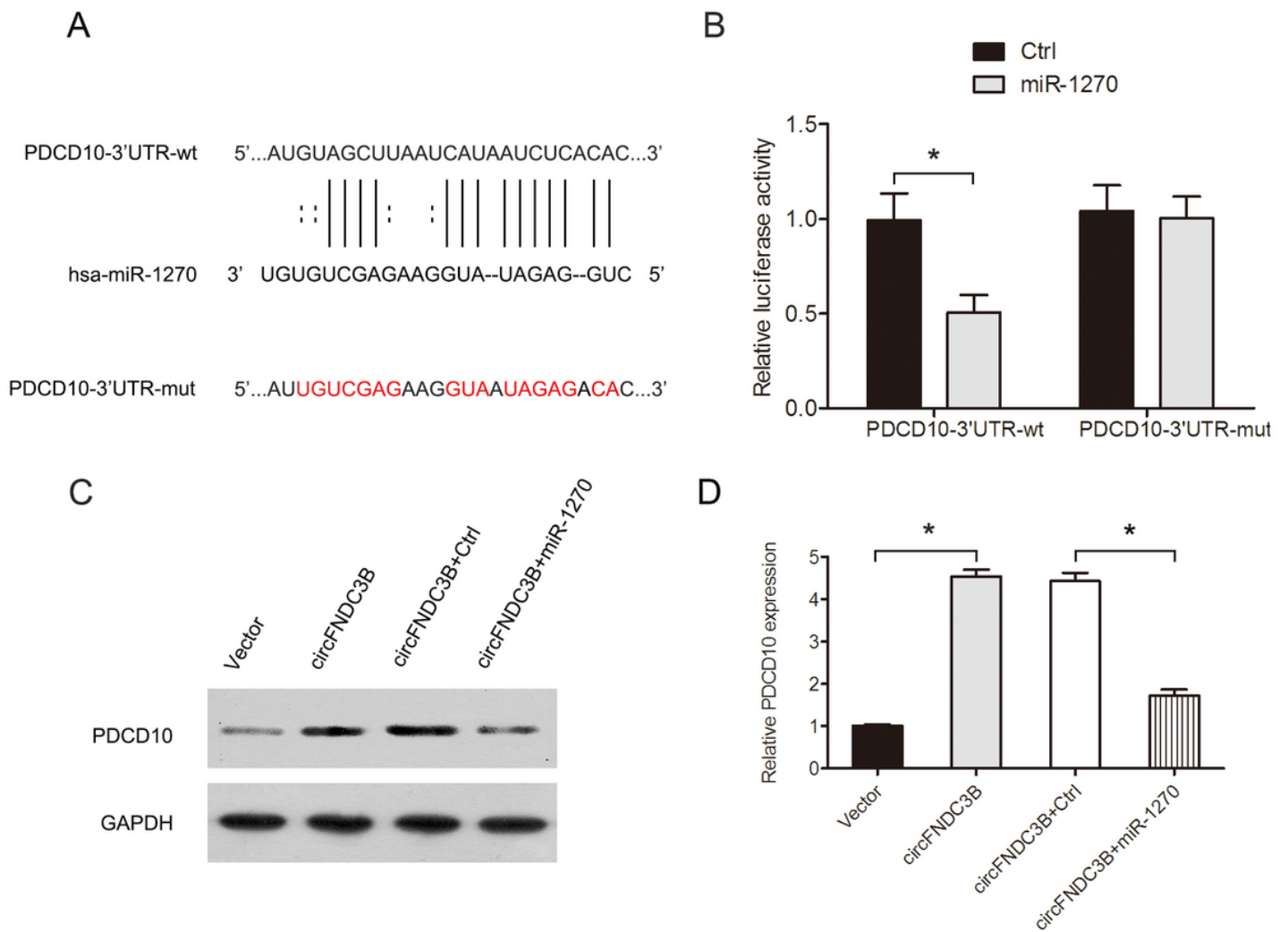


Figure 5

PDCD10 expression is inhibited by circFNDC3B through by sponging miR-1270. a The binding site of miR-1270 and PDCD10 3'UTR. b Luciferase activity in VSMCs after co-transfection with wild type or mutant PDCD10 3'UTR reporter and miR-1270 or control mimics. c-d The expression of PDCD10 protein and mRNA levels were detected by qRT-PCR and western blot, respectively. Values represent the mean \pm SD (n = 3 per group). *p < 0.05.

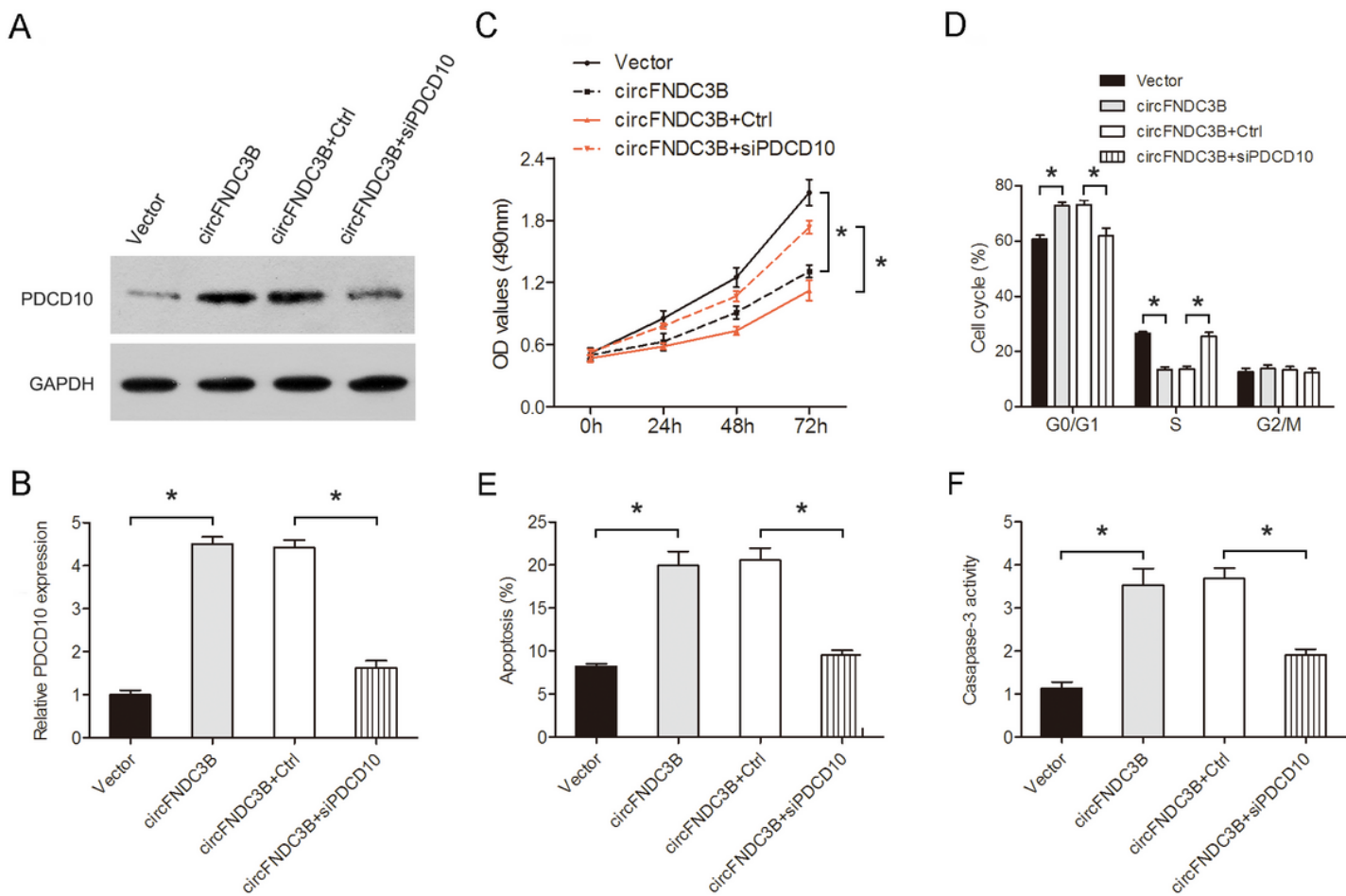


Figure 6

CircFNDC3B inhibits VSMC proliferation and enhances apoptosis via the miR-1270/PDCD10 axis. a-b VSMCs were co-transfected with circFNDC3B plasmid and siPDCD10, and qRT-PCR and western blot were performed to test the expression of PDCD10 mRNA and protein, respectively. c-f VSMC proliferation, cell cycle progression, and apoptosis were examined using MTT, flow cytometry, and caspase-3 activity assays. Values represent the mean \pm SD (n = 3 per group). *p < 0.05.

Supplementary Files

This is a list of supplementary files associated with this preprint. Click to download.

- [Table1.xlsx](#)
- [SupplementaryMaterial.docx](#)